

## Intersubband transitions in bismuth nanowires

M. R. Black<sup>a)</sup>

*Department of Electrical Engineering and Computer Science, Massachusetts Institute of Technology, Cambridge, Massachusetts 02139-4307*

M. Padi and S. B. Cronin

*Department of Physics, Massachusetts Institute of Technology, Cambridge, Massachusetts 02139-4307*

Y.-M. Lin

*Department of Electrical Engineering and Computer Science, Massachusetts Institute of Technology, Cambridge, Massachusetts 02139-4307*

O. Rabin

*Department of Chemistry, Massachusetts Institute of Technology, Cambridge, Massachusetts 02139-4307*

T. McClure

*The Center For Material Science and Engineering, Massachusetts Institute of Technology, Cambridge, Massachusetts 02139-4307*

G. Dresselhaus

*Francis Bitter Magnet Laboratory, Massachusetts Institute of Technology, Cambridge, Massachusetts 02139-4307*

P. L. Hagelstein and M. S. Dresselhaus<sup>b)</sup>

*Department of Electrical Engineering and Computer Science, Massachusetts Institute of Technology, Cambridge, Massachusetts 02139-4307*

(Received 25 September 2000; accepted for publication 18 October 2000)

Optical absorption associated with the one-dimensional joint density of states of an intersubband transition in bismuth nanowires is reported. The previously observed strong absorption in bismuth nanowires at  $\sim 1000 \text{ cm}^{-1}$  is here shown to depend on the wire diameter and on the polarization of the incident light. The absorption line shape, the decreasing frequency with increasing wire diameter, and the polarization dependence of the reflectivity, all indicate that this resonance is due to an intersubband absorption resulting from quantum-confinement effects. © 2000 American Institute of Physics. [S0003-6951(00)05351-1]

Recent research has focused on low-dimensional structures as another way to control the properties of materials. Quantum dots, wires,<sup>1</sup> and wells are being investigated for potential applications, such as memory media,<sup>2</sup> high-speed electronics, optical devices,<sup>3</sup> and thermoelectric materials.<sup>4,5</sup> However, in order to better tailor low-dimensional structures to a particular application, the effects of quantum confinement on the system need to be well understood. This letter studies intersubband optical transitions in bismuth nanowires as a way of building this understanding.

When the sample size is smaller than the mean free path and the de Broglie wavelength of the conduction electrons, then the electrons are quantum confined, and the electronic bands split into subbands. In order to have a measurable energy separation between subbands, a large mean free path and a small effective mass (a long electron wavelength) are desired. We have studied bismuth nanowires here because Bi has both of these desired properties. Bulk bismuth, a semimetal, has a very anisotropic effective electron mass tensor, with mass components  $\mathbf{m}^*$  varying from  $0.001 m_0$  to  $0.26 m_0$ , depending on the crystalline direction. Crystalline bismuth also has a mean free path of  $\sim 250 \text{ nm}$  at  $300 \text{ K}$ .<sup>6</sup>

Moreover, bismuth nanowires are especially interesting because they exhibit a transition from a semimetal with a small band overlap (38 meV at 0 K) to a semiconductor, as the wire size becomes small enough to support significant quantum confinement effects.<sup>7</sup> This transition occurs in Bi nanowires at relatively large wire diameters because of its small effective masses and small band overlap. For example, this transition is predicted to occur at a wire diameter of 48 nm in the (202) direction (the growth direction of our nanowires). The change from a semimetal to a semiconductor has significant effects on the electronic properties of bismuth, which may be desirable for some applications. Finally, bismuth has a low melting point ( $\sim 271 \text{ }^\circ\text{C}$ ), which makes it compatible with our pressure injection technique for fabricating nanowires.

The bismuth nanowires used in this study are fabricated inside the pores of anodic alumina,<sup>8,9</sup> which serves as a host material. Since alumina is a wide-band gap semiconductor, individual wires are therefore electrically isolated.

For Bi inside the nanopores of alumina templates, quantum-confinement effects become important, and the direct ( $L$ -point) interband transition energy increases with decreasing nanowire diameter. The plasma frequency is smaller in nanowires than in bulk materials due to the lower carrier concentration, although the low dielectric constant of the alumina reduces the magnitude of this effect. As the wire diam-

<sup>a)</sup>Electronic mail: mrb@mgt.mit.edu

<sup>b)</sup>Also at: Dept. of Physics, MIT; currently on leave from MIT.

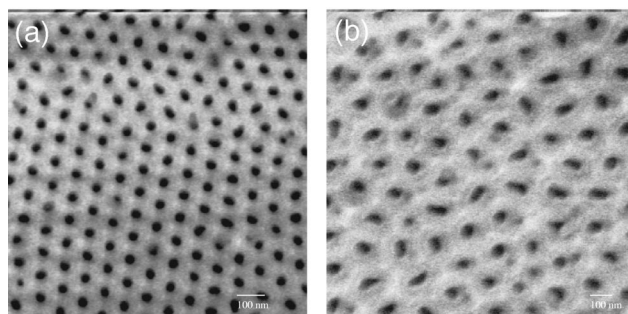


FIG. 1. Scanning electron microscope images of samples 2 (a) and 4 (b). Sample 4 has a narrow distribution of wire diameters around 35 nm while sample 2 has a wide distribution of wire diameters around  $\sim 70$  nm.

eter decreases, the plasma frequency is expected to decrease slightly as a result of the increased band gap. In bulk bismuth, the direct band gap ( $L$ -point) transition and free carrier plasmon frequencies occur at 290 (36 meV) and 333  $\text{cm}^{-1}$  (41.3 meV), respectively. For undoped 40 nm bismuth wires at 293 K, for example, a direct band gap of approximately 990  $\text{cm}^{-1}$  and a plasma frequency  $\sim 210$   $\text{cm}^{-1}$  are expected (using an effective mass of 0.5, a calculated carrier concentration of  $1.6 \times 10^{18} \text{ cm}^{-3}$ , and a measured dielectric constant  $\epsilon = 4$ ). Since our measurements are made in the frequency range 650–4000  $\text{cm}^{-1}$ , we expect to observe an allowed interband transition, but not the free carrier plasmon absorption. In the frequency range of our experiments, the wavelength of light is more than 50 times greater than the wire diameter. As a result, both the alumina host material and the bismuth nanowires contribute to the measured optical properties. The contributions of the nanowires can be separated from that of the measured nanowire/dielectric composite by use of an effective medium theory formalism.<sup>10–13</sup>

In a material that is quantum confined in two dimensions (quantum wires), the joint electronic density of states has a singularity at each energy corresponding to an allowed intersubband transition, which may result in a large absorption at this energy. In this study, we report optical absorption associated with these transitions.

Porous anodic aluminum oxide templates are fabricated by anodizing aluminum sheets in an oxalic acid solution.<sup>8</sup> During this process, cylindrical pores 7–200 nm in diameter are self-assembled into a hexagonal array, as shown in Fig. 1. The pore diameter and the distance between the pores can be controlled systematically by varying the anodization voltage and the electrolyte used.<sup>14,15</sup> The process conditions for the four samples used in this study are listed in Table I. Scanning electron micrographs of samples 2 and 3 are shown in Fig. 1. The pores in the alumina templates are filled with Bi using a pressure injection technique.<sup>8</sup>

TABLE I. Sample processing conditions.

Sample	Voltage (V)	Temperature (K)	Wire diameter (nm)	Purity of Bi used to fill template (%)
1	60	273	65–80	99.99
2	60	275	$\sim 70$	99.999
3	40	290	55	99.999
4	35	273	35	99.999

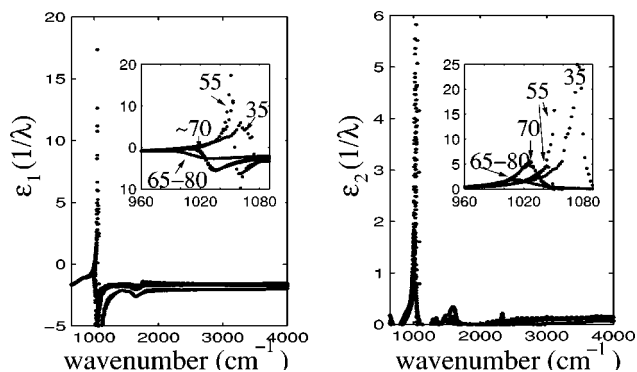


FIG. 2. The dielectric function ( $\epsilon_1 + i\epsilon_2$ ) of bismuth nanowires vs wave number ( $1/\lambda \text{ cm}^{-1}$ ) obtained from analysis of reflectivity measurements for samples 1, 2, 3, and 4, which are determined from the corresponding reflectivity spectra by analysis of the effect of the alumina host material. Two measurements on samples 2 and 3 from different locations on the sample are shown in the inserted figures to demonstrate the reproducibility of the results.

The optical reflection  $R(\omega)$  and transmission  $T(\omega)$  were measured as a function of frequency at room temperature using a Nicolet Magna-IR 860 spectrometer and the Nic-Plan IR Microscope. Reflection data were taken in the infrared region from  $650 < 1/\lambda < 4000 \text{ cm}^{-1}$  at 293 K using a gold film as a comparison standard. In both measurements, the resolution was 4  $\text{cm}^{-1}$ .

The frequency-dependent reflectivity of samples (1–4) in Table I was measured for incident light directed parallel to the wire axis. With this sample orientation, the electric field is always perpendicular to the wire axis, even for unpolarized light, and therefore intersubband transitions may occur. Using Kramers–Kronig relations and the reflection versus wavenumber, the dielectric constant for the composite material is obtained as a function of energy. The dielectric function of nonporous alumina is obtained using effective medium theory with the aid of the dielectric function of an unfilled alumina template, and the measured porosity of the alumina.<sup>16</sup> Again applying effective medium theory, the contribution to the dielectric function of the alumina host is deduced from the dielectric function of the bismuth/alumina composite, and the dependence of the dielectric function of the bismuth nanowires on wavenumber ( $1/\lambda$ ) is determined.<sup>16</sup> Results thus obtained for the dielectric function [ $\epsilon_1(1/\lambda) + i\epsilon_2(1/\lambda)$ ] of bismuth nanowires from samples 1–4 are shown in Fig. 2 as a function of wave number ( $1/\lambda$ ).

In Fig. 2, a resonance at  $\sim 1000 \text{ cm}^{-1}$  is observed for all samples. Since the wire diameters of samples 1 (65–80 nm) and 2 ( $\sim 70$  nm) are larger than the wire diameters of samples 3 (55 nm) and 4 (35 nm), the intersubband transition energies for samples 1 and 2 are predicted to be smaller, in qualitative agreement with the observed shift of the absorption peak energy as seen in the insets of Fig. 2.

The reflection spectra for light incident from the side of a bismuth-filled template are shown in Fig. 3. Curve (f) shows the frequency-dependent reflectivity (versus  $1/\lambda$ ) for the incident light, polarized perpendicular to the wire axis ( $\theta = 0^\circ$ ), while curve (a) is for light polarized parallel to the wire axis ( $\theta = 90^\circ$ ). The reflectivity spectra for incident light polarized at  $\pm 27^\circ$  away from the high-symmetry directions are also shown in curves (b)–(e).

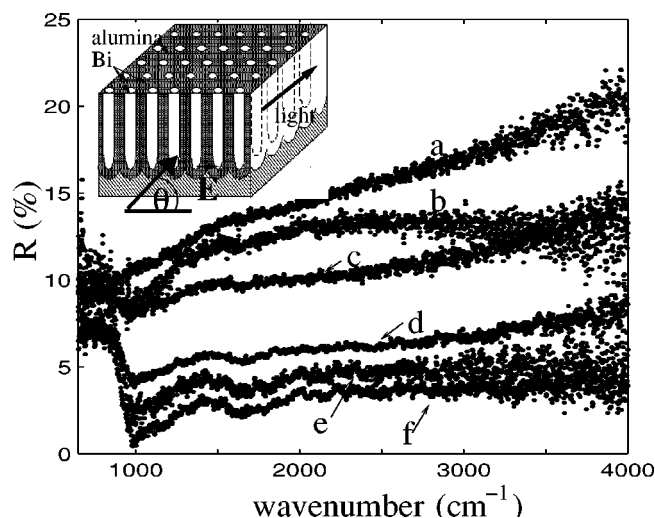


FIG. 3. Reflection [ $R(1/\lambda)$ ] of a Bi filled sample with several polarization angles  $\theta$ : (a)  $90^\circ$ , (b)  $117^\circ$ , (c)  $63^\circ$ , (d)  $27^\circ$ , (e)  $-27^\circ$ , (f)  $0^\circ$ . Curve (f) ( $\theta=0^\circ$ ) shows features around  $1000\text{ cm}^{-1}$ , while curve (a) ( $\theta=90^\circ$ ) does not exhibit clear features in this region, consistent with the selection rules for an intersubband transition.

As curve (a) in Fig. 3 demonstrates, the reflectivity of the filled sample when the light is polarized parallel to the wire axis does not exhibit strong features in the  $\sim 1000\text{ cm}^{-1}$  frequency range. For the light polarized parallel to the wire axis ( $\theta=90^\circ$ ), we do not expect to see any intersubband transitions, since in this case, the electric field is uniform in the quantum-confined direction. Therefore, the electromagnetic dipole matrix element between the valence and conduction states  $\langle v | (e/mc) \mathbf{p} \cdot \mathbf{A}_{\text{light}} | c \rangle$  vanishes, and no electromagnetic coupling occurs between the conduction and valence bands. In addition, when the light is polarized parallel to the wire axis, the reflection is dominated by the free carriers contributing to the reflectivity.

A change in polarization, however, causes the appearance of absorption bands in the reflection spectrum of the filled sample [see Figs. 3(b)–3(f)]. This polarization-dependent absorption was not detected for unfilled alumina templates, indicating that this feature is indeed caused by the presence of the Bi nanowires. When the light is polarized perpendicular to the wire axis ( $\theta=0^\circ$ ), the valence and conduction bands may be coupled through the electromagnetic interaction which couples the momentum of the electrons to the vector potential of the light. Thus, we expect to observe an interband resonator at  $\sim 1000\text{ cm}^{-1}$  for light polarized perpendicular to the wire axis, consistent with observations. Previously, an oscillator at  $1000\text{ cm}^{-1}$  in bismuth nanowires

was tentatively assigned to an intersubband transition.<sup>16</sup> The disappearance of this feature when the light is polarized parallel to the wires (see Fig. 3) corroborates the earlier preliminary assignment, suggesting that this resonator is indeed due to an intersubband transition.

This letter reports a strong oscillator absorption in bismuth nanowires at  $\sim 1000\text{ cm}^{-1}$ . The absorption is observed for light polarized perpendicular to the wire axis and is absent for light polarized parallel to the wire axis. In addition, the oscillator is observed to increase in energy with decreasing wire diameter size, consistent with the energy shift due to quantum confinement. The energy of the resonance, the polarization anisotropy of the absorption, as well as the wire diameter dependence, all strongly suggest that this resonator is an intersubband absorption via optical measurements.

The authors gratefully acknowledge MURI Subcontract No. 0205-G-7A114-01, NSF Grant No. DMR-98-04734, and US Navy Contract No. N00167-92-K005 for support. This work made use of MRSEC Shared Facilities supported by the National Science Foundation Contract No. DMR-9400334.

- <sup>1</sup>M. S. Sander, R. Gronsky, Y.-M. Lin, and M. S. Dresselhaus, *J. Appl. Phys.* (in press).
- <sup>2</sup>N. Kouklin, S. Bandyopadhyay, S. Tereshin, A. Varfolomeev, and D. Zaretsky, *Appl. Phys. Lett.* **76**, 460 (2000).
- <sup>3</sup>D. E. Aspnes, A. Heller, and J. D. Porter, *J. Appl. Phys.* **60**, 3028 (1986).
- <sup>4</sup>M. S. Dresselhaus, T. Koga, X. Sun, S. B. Cronin, K. L. Wang, and G. Chen, in *Sixteenth International Conference on Thermoelectrics: Proceedings, ICT'97; August 26–29, 1997, Dresden, Germany*, edited by A. Heinrich and J. Schumann (Institute of Electrical and Electronics Engineers, Inc., Piscataway, NJ, 1997), pp. 12–20.
- <sup>5</sup>L. D. Hicks and M. S. Dresselhaus, *Phys. Rev. B* **47**, 12 727 (1993).
- <sup>6</sup>V. Damodara Das and N. Soundararajan, *Phys. Rev. B* **35**, 5990 (1987).
- <sup>7</sup>Y. M. Lin, X. Sun, and M. S. Dresselhaus, *Phys. Rev. B* **62**, 4610 (2000).
- <sup>8</sup>Z. Zhang, J. Ying, and M. Dresselhaus, *J. Mater. Res.* **13**, 1745 (1998).
- <sup>9</sup>J. Heremans, C. M. Thrush, Y. Lin, S. Cronin, Z. Zhang, M. S. Dresselhaus, and J. F. Mansfield, *Phys. Rev. B* **61**, 2921 (2000).
- <sup>10</sup>G. L. Hornyak, C. J. Patrissi, and C. R. Martin, *J. Phys. Chem. B* **101**, 1548 (1997).
- <sup>11</sup>C. A. Foss, Jr., G. L. Hornyak, J. A. Stockert, and C. R. Martin, *J. Phys. Chem. B* **98**, 2963 (1994).
- <sup>12</sup>D. E. Aspnes, *Thin Solid Films* **89**, 249 (1982).
- <sup>13</sup>N. L. Cherkas, *Opt. Spectrosc.* **81**, 906 (1996).
- <sup>14</sup>J. W. Diggle, T. C. Downie, and C. W. Goulding, *Chem. Rev.* **69**, 365 (1969).
- <sup>15</sup>J. P. Sullivan and G. C. Wood, *Proc. R. Soc. London, Ser. A* **317**, 511 (1970).
- <sup>16</sup>M. R. Black, Y.-M. Lin, M. S. Dresselhaus, M. Tachibana, S. Fang, O. Rabin, F. Ragot, P. C. Eklund, and Bruce Dunn, in *Nanophase and Nanocomposite Materials III: MRS Symposium Proceedings, Boston, November 29–December 3, 1999*, edited by S. Komarenii, J. C. Parker, and H. Hahn (Materials Research Society, Pittsburgh, PA, 2000).